Physics Letters B 835 (2022) 137580

Contents lists available at ScienceDirect

Physics Letters B

journal homepage: www.elsevier.com/locate/physletb

Target normal single-spin asymmetry in inclusive electron-nucleon scattering with two-photon exchange: Analysis using $1/N_c$ expansion

J.L. Goity [a,b], C. Weiss [b,*], C.T. Willemyns [c]

[a] Department of Physics, Hampton University, Hampton, VA 23668, USA
[b] Theory Center, Jefferson Lab, Newport News, VA 23606, USA
[c] Service de Physique Nucléaire et Subnucléaire, Université de Mons, UMONS Research Institute for Complex Systems, Place du Parc 20, 7000 Mons, Belgium

ARTICLE INFO

Article history:
Received 30 July 2022
Accepted 16 November 2022
Available online 21 November 2022
Editor: J.-P. Blaizot

ABSTRACT

We calculate the target normal single-spin asymmetry caused by two-photon exchange in inclusive electron-nucleon scattering in the resonance region. Our analysis uses the $1/N_c$ expansion of low-energy QCD and combines N and Δ intermediate and final states using the contracted $SU(4)$ spin-flavor symmetry. The normal spin asymmetry obtained in leading-order accuracy in $1/N_c$ has magnitude $\sim 10^{-2}$ and different sign in *ep* and *en* scattering. It can be measured in electron scattering at lab energies $\sim$0.5–1.5 GeV and provides a clean probe of two-photon exchange dynamics.

1. Introduction

Electron scattering represents a principal tool for exploring hadron structure and strong interaction dynamics. The process is traditionally described in leading order of the electromagnetic coupling (one-photon exchange approximation), where the amplitude is proportional to the transition matrix element of the electromagnetic current operator between the hadronic states. Recent developments in experiment and theory point to the need of including higher-order interactions between the electron and the hadronic system (two-photon exchange) in certain observables [1]. Measurements of the proton form factor ratio G_E^p/G_M^p at Jefferson Lab using the Rosenbluth separation and polarization transfer methods show discrepancies that have been associated with two-photon exchange [2–4]. A direct demonstration of two-photon exchange becomes possible through comparison of electron and positron scattering in experiments at DESY [5,6] and Jefferson Lab [7]. Two-photon exchange is also discussed in connection with muon scattering at MUSE [8] and plays an important role in radiative corrections to parity-violating electron scattering [9]. Two-photon exchange has thus become as field of research in its own right.

A particularly interesting observable is the target spin dependence in inclusive electron-nucleon scattering,

$$e(k_\mathrm{i}) + N\!\uparrow\!(p_\mathrm{i}, a_\mathrm{i}) \to e(k_\mathrm{f}) + X(p_\mathrm{f}), \tag{1}$$

where X denotes the hadronic final states accessible at the incident energy, which are summed over. If the electron is unpolarized, and the nucleon is polarized with a spin 4-vector a_i, with $a_\mathrm{i}^2 = -1$ for complete polarization, the dependence of the differential cross section on the nucleon spin is of the form [10]

$$\frac{d\sigma}{d\Gamma_\mathrm{f}} = \frac{d\sigma_U}{d\Gamma_\mathrm{f}} - e_N^\mu a_{\mathrm{i}\mu} \frac{d\sigma_N}{d\Gamma_\mathrm{f}} \tag{2}$$

($d\Gamma_\mathrm{f}$ denotes the invariant phase space element of the final electron and will be specified below). Here e_N is the normalized pseudovector formed from the initial and final electron momenta and the initial nucleon momentum ($\epsilon^{0123} = 1$),

$$e_N^\mu \equiv \frac{N^\mu}{\sqrt{-N^2}}, \quad N^\mu \equiv -\epsilon^{\mu\alpha\beta\gamma} p_{\mathrm{i}\alpha} k_{\mathrm{f}\beta} k_{\mathrm{i}\gamma}, \quad e_N^2 = -1. \tag{3}$$

In the nucleon rest frame, $\boldsymbol{p}_\mathrm{i} = 0$, the spin 4-vector is $a_\mathrm{i} = (0, 2\boldsymbol{S}_\mathrm{i})$, with $|\boldsymbol{S}_\mathrm{i}| = 1/2$ for complete polarization, and e_N is the normal vector to the scattering plane, so that the cross section Eq. (2) depends on the normal component of the nucleon spin,

$$e_N = (0, \boldsymbol{e}_N), \quad \boldsymbol{e}_N = \frac{\boldsymbol{k}_\mathrm{f} \times \boldsymbol{k}_\mathrm{i}}{|\boldsymbol{k}_\mathrm{f} \times \boldsymbol{k}_\mathrm{i}|}, \quad -e_N^\mu a_{\mathrm{i}\mu} = 2\boldsymbol{e}_N \cdot \boldsymbol{S}_\mathrm{i} \tag{4}$$

[this form applies in any frame where the 3-momenta $\boldsymbol{k}_\mathrm{i}, \boldsymbol{k}_\mathrm{f}$ and $\boldsymbol{p}_\mathrm{i}$ lie in a plane, e.g. the electron-nucleon center-of-mass (CM) frame, where $\boldsymbol{p}_\mathrm{i} + \boldsymbol{k}_\mathrm{i} = 0$]. The spin-dependent cross section in Eq. (2) is zero in one-photon exchange approximation, as a consequence of P and T invariance, and represents a pure two-photon exchange observable [11,12]. It is proportional to the imaginary (absorptive)

* Corresponding author.
E-mail addresses: goity@jlab.org (J.L. Goity), weiss@jlab.org (C. Weiss), cintiawillemyns@gmail.com (C.T. Willemyns).

https://doi.org/10.1016/j.physletb.2022.137580

part of the $eN \to eX$ two-photon exchange amplitude, which is given by the product of on-shell matrix elements between the initial, intermediate, and final electron-hadron states. Unlike the real (dispersive) part, the imaginary part of the two-photon exchange amplitude is infrared–finite and can be considered separately from real photon emission into the final state [10].

Measurements of the normal spin asymmetry (the ratio of the N and U cross sections) have been performed in deep-inelastic electron scattering (DIS) on proton [13] and ^{3}He targets [14]. Theoretical calculations in this kinematics have employed the parton picture and QCD interactions and produced a wide range of estimates [10,15–17]. Further measurements at few-GeV energies are planned at Jefferson Lab [18]. Calculations in the resonance region need to account for the contributions of individual hadronic channels to the inclusive cross section, including elastic scattering and resonance excitation, and require appropriate methods.

In this work we analyze the normal spin dependence of inclusive eN scattering in the resonance region using the $1/N_c$ expansion. The method organizes low-energy dynamics (hadron masses, couplings, form factors) based on the scaling properties in the limit of a large number of colors in QCD and has been successfully applied in many areas of hadronic physics [19–25]. Low-lying baryon states are organized in multiplets of the emerging contracted $SU(4)$ spin-flavor symmetry, with the baryon masses $O(N_c)$ and the splitting inside multiplets $O(N_c^{-1})$. The ground-state multiplet contains the N and Δ, and transitions between them are governed by the symmetry and can be computed using group-theoretical techniques, with the parameters for the N–Δ and Δ–Δ transitions fixed in terms of the measurable N–N transitions.

The $1/N_c$ expansion offers specific advantages for studying two-photon exchange in inclusive scattering. The method treats N and Δ states on the same basis and enables a consistent description of inelastic channels and inclusive scattering in the resonance region. The group-theoretical techniques permit efficient calculation of the sums over channels in intermediate and final states. The parametric ordering of the kinematic variables gives rise to a physical picture that enables an intuitive understanding of the two-photon exchange process.

In this letter we present the leading-order $1/N_c$ expansion and describe the calculational techniques and physical picture specific to this situation. A full analysis, including $1/N_c$ corrections and suppressed structures, will be presented in a forthcoming article.

2. Method

2.1. Kinematics and final states

Inclusive electron scattering Eq. (1) is characterized by three independent kinematic variables, corresponding to the incident energy, the momentum transfer, and the energy transfer of the process. They can be chosen as the invariant variables

$$s \equiv (k_\mathrm{i} + p_\mathrm{i})^2 = (k_\mathrm{f} + p_\mathrm{f})^2, \tag{5}$$

$$t \equiv (k_\mathrm{i} - k_\mathrm{f})^2 = (p_\mathrm{f} - p_\mathrm{i})^2 = q^2, \tag{6}$$

$$m_X^2 = (q + p_\mathrm{i})^2 = p_\mathrm{f}^2, \tag{7}$$

where $q \equiv k_\mathrm{i} - k_\mathrm{f} = p_\mathrm{f} - p_\mathrm{i}$ is the 4-momentum transfer. In the following we use the CM frame, where the 3-momenta in the initial and final states are $\boldsymbol{p}_\mathrm{i} = -\boldsymbol{k}_\mathrm{i}$, $\boldsymbol{p}_\mathrm{f} = -\boldsymbol{k}_\mathrm{f}$, with

$$|\boldsymbol{k}_\mathrm{i}| = \frac{s - m^2}{2\sqrt{s}}, \qquad |\boldsymbol{k}_\mathrm{f}| = \frac{s - m_X^2}{2\sqrt{s}}, \tag{8}$$

$$t = -2|\boldsymbol{k}_\mathrm{f}||\boldsymbol{k}_\mathrm{i}|(1 - \cos\theta), \qquad \theta \equiv \mathrm{angle}(\boldsymbol{k}_\mathrm{f}, \boldsymbol{k}_\mathrm{i}), \tag{9}$$

where m is the nucleon mass.

When analyzing the process Eq. (1) in the $1/N_c$-expansion, we have to specify the scaling behavior of the kinematic variables in the parameter $1/N_c$. Different choices are possible, leading to different types of expansions. Here we consider the domain where the initial and final CM momenta are

$$|\boldsymbol{k}_\mathrm{i}|, |\boldsymbol{k}_\mathrm{f}| \;=\; O(N_c^0), \tag{10}$$

corresponding to $\sqrt{s} = O(N_c)$ and $\sqrt{s} - m = O(N_c^0)$. For the final-state masses we consider values such that

$$m_X - m \;=\; O(N_c^{-1}), \qquad m, m_X \;=\; O(N_c). \tag{11}$$

In this domain the only accessible final states are the ground-state baryon multiplet containing the N and Δ states, $X = N + \Delta$; other baryon multiplets have masses $m_X - m = O(N_c^0)$ and are not accessible as final states. Together, Eqs. (10) and (11) imply

$$|\boldsymbol{k}_\mathrm{i}| - |\boldsymbol{k}_\mathrm{f}| \;=\; \frac{m_X^2 - m^2}{2\sqrt{s}} \;=\; O(N_c^{-1}) \;\ll\; |\boldsymbol{k}_\mathrm{f}|, |\boldsymbol{k}_\mathrm{i}|. \tag{12}$$

In leading order of $1/N_c$ we can therefore neglect the difference between $|\boldsymbol{k}_\mathrm{i}|$ and $|\boldsymbol{k}_\mathrm{f}|$ and use the common CM momentum

$$k \;\equiv\; |\boldsymbol{k}_\mathrm{i}| \;=\; |\boldsymbol{k}_\mathrm{f}| + O(N_c^{-1}). \tag{13}$$

For the CM scattering angle we consider values $\theta = O(N_c^0)$, which together with Eq. (10) implies

$$t = O(N_c^0). \tag{14}$$

The parametric ordering in $1/N_c$ adopted here gives rise to a definite physical picture of the scattering process. The electron with energy $O(N_c^0)$ scatters from the heavy nucleon with mass $O(N_c)$, losing a small fraction $O(N_c^{-1})$ of its energy. The nucleon remains intact or gets excited to a Δ by absorbing a small energy $O(N_c^{-1})$. The velocity of the initial/final baryons is small $O(N_c^{-1})$, and their kinetic energy is negligible compared to the electron energy. However, the momentum transfer is $O(N_c^0)$, so that the process probes the internal structure of the baryons.

In the parametric domain considered here, inelastic scattering consists simply in the transition from N to Δ states, which can be regarded as stable in leading order of $1/N_c$ (the Δ width is suppressed). This corresponds to the physical situation that πN final states are predominantly produced through Δ resonance decay. Non-resonant πN states do not appear explicitly at leading order in $1/N_c$ in the domain considered here.

2.2. Currents and amplitudes

In the group-theoretical formulation of large-N_c QCD, the N and Δ are states in the $SU(4)$ multiplet of ground-state baryons, characterized by the spin/isospin $S = I = 1/2$ and $3/2$, the spin projection S_3, and the isospin projection I_3, denoted collectively by $B \equiv \{S, S_3, I_3\}$. The electron scattering process takes the form of a transition between baryon states $\langle B_\mathrm{f}|...|B_\mathrm{i}\rangle$. We denote the electron-baryon scattering amplitude by

$$M(k, \boldsymbol{n}_\mathrm{f}, \boldsymbol{n}_\mathrm{i}|\lambda, B_\mathrm{f}, B_\mathrm{i}) \;\equiv\; M_\mathrm{fi}, \tag{15}$$

where k is the common CM momentum Eq. (13), and

$$\boldsymbol{n}_\mathrm{i} \equiv \boldsymbol{k}_\mathrm{i}/|\boldsymbol{k}_\mathrm{i}|, \qquad \boldsymbol{n}_\mathrm{f} \equiv \boldsymbol{k}_\mathrm{f}/|\boldsymbol{k}_\mathrm{f}| \tag{16}$$

are the unit vectors along the initial/final electron CM momenta. In our convention the electron states have covariant normalization, while the baryon states have non-covariant normalization; in this way the baryon mass does not appear in the expressions for the

phase space integral Eq. (25) and cross section Eq. (26), which is natural for the $1/N_c$ expansion. In Eq. (15), λ is the electron helicity (spin projection on $\boldsymbol{n}_\mathrm{i}$ and $\boldsymbol{n}_\mathrm{f}$), which is conserved in the scattering process. The baryon spins are quantized along a fixed direction in the CM frame; in this way the initial and final states have the same quantization axis, and the spin transitions can be computed using algebraic identities [24,25].[1]

The amplitude Eq. (15) can be computed as an expansion in the electromagnetic coupling,

$$M_\mathrm{fi} = M_\mathrm{fi}^{(e2)} + M_\mathrm{fi}^{(e4)} + \dots \tag{17}$$

The e^2 term (one-photon exchange) is given by the product of the electron and baryon currents,

$$M_\mathrm{fi}^{(e2)} = -\frac{e^2}{t_\mathrm{fi}} (j^\mu)_\mathrm{fi} (J_\mu)_\mathrm{fi}, \tag{18}$$

$$t_\mathrm{fi} = -2k^2 (1 - \boldsymbol{n}_\mathrm{f}\boldsymbol{n}_\mathrm{i}), \tag{19}$$

$$(j^\mu)_\mathrm{fi} = \bar{u}(\boldsymbol{n}_\mathrm{f}, \lambda)\, \gamma^\mu\, u(\boldsymbol{n}_\mathrm{i}, \lambda), \tag{20}$$

$$(J^\mu)_\mathrm{fi} = \langle -\boldsymbol{n}_\mathrm{f}, B_\mathrm{f} | \hat{J}^\mu | -\boldsymbol{n}_\mathrm{i}, B_\mathrm{i} \rangle. \tag{21}$$

The minus sign in Eq. (18) comes from the negative electric charge of the electron. The electron current Eq. (20) is the standard current of the spin-1/2 particle; its explicit form can be derived from the spinors in the CM frame. The baryon current Eq. (21) can be constructed using the large-N_c $SU(4)$ spin-flavor symmetry and expanded in the generators $\{\hat{1}, \hat{I}^a, \hat{S}^i, \hat{G}^{ia}\} (i, a = 1, 2, 3)$ [24–26]. Their matrix elements are of the order

$$\langle B_\mathrm{f} | \{\hat{1}, \hat{I}^a, \hat{S}^i\} | B_\mathrm{i} \rangle = O(N_c^0), \qquad \langle B_\mathrm{f} | \hat{G}^{ia} | B_\mathrm{i} \rangle = O(N_c). \tag{22}$$

The full $1/N_c$ expansion of the current is given in Ref. [26]. In the present study we focus on the leading-order contribution to the cross sections, which is produced by the isovector magnetic current proportional to $\hat{G}^{i3}$. This current is given by

$$(J^0)_\mathrm{fi} = 0, \quad (J^i)_\mathrm{fi} = ik\epsilon^{ijk} (n_\mathrm{f} - n_\mathrm{i})^j \langle B_\mathrm{f} | \hat{G}^{k3} | B_\mathrm{i} \rangle\, F(t_\mathrm{fi}). \tag{23}$$

It satisfies the transversality condition $q^\mu (J_\mu)_\mathrm{fi} = 0$ for all transitions between multiplet states, without corrections in $1/N_c$.

The function $F(t)$ in Eq. (23) (dimension mass^{-1}) is the large-N_c form factor, which describes the dynamical response of the large-N_c baryon to the momentum transfer $t = O(N_c^0)$. It can be determined by matching the $N \to N$ matrix element of the large-N_c current Eq. (23) with the physical nucleon current at $N_c = 3$. At leading order in $1/N_c$ one obtains

$$F(t) = \left. \frac{G_M^V(t)}{m} \right|_\mathrm{phys}, \tag{24}$$

where $G_M^V(t) \equiv \frac{1}{2}[G_M^p(t) - G_M^n(t)]$ is the physical nucleon isovector magnetic form factor, whose value at $t = 0$ is given by the proton and neutron magnetic moments, $G_M^V(0) = \frac{1}{2}(\mu^p - \mu^n)$, and m is the physical nucleon mass. In this way the spin-flavor symmetry fixes the N–Δ and Δ–Δ form factors in terms of the empirical N–N form factor, showing the predictive power of the $1/N_c$ expansion.

[1] The following calculation does not refer to a specific coordinate system. For definiteness we can imagine using a system where $\boldsymbol{n}_\mathrm{f} + \boldsymbol{n}_\mathrm{i}$ defines the $+x$-direction, and $\boldsymbol{n}_\mathrm{f} - \boldsymbol{n}_\mathrm{i}$ the $+z$-direction, and quantize the baryon spin along the $+z$-direction; in this system the normal vector $\boldsymbol{e}_N$, Eq. (4), points in the $+y$ direction, and the spin density matrix Eq. (28) is $\sigma^y/2$.

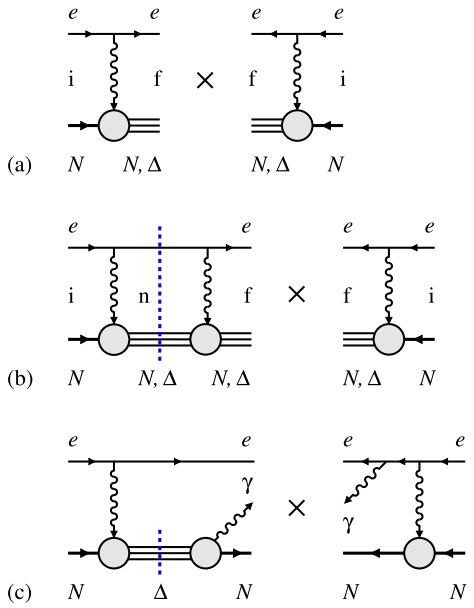

Fig. 1. Inclusive eN scattering in the $1/N_c$ expansion in the domain Eqs. (10) and (11). (a) Spin-independent cross section from square of e^2 amplitudes. (b) Spin-dependent cross section from interference of e^4 and e^2 amplitudes. It includes also the complex-conjugate term, in which the e^4 and e^2 amplitudes are interchanged (not shown here). (c) Interference of real photon emission from electron and baryon.

The e^4 term in the electron-baryon scattering amplitude Eq. (17) results from two-photon exchange interactions. The absorptive part arises from on-shell rescattering and can be computed as the product of two e^2 amplitudes, integrated over the phase space of the intermediate state (see Fig. 1b),

$$M_\mathrm{fi}^{(e4)} = \frac{ik}{4\pi} \int \frac{d\Omega_\mathrm{n}}{4\pi} \sum_{B_\mathrm{n}} M_\mathrm{fn}^{(e2)} M_\mathrm{ni}^{(e2)}. \tag{25}$$

We use the shorthand notation Eq. (15) for the amplitudes of the $\mathrm{i} \to \mathrm{n}$ and $\mathrm{n} \to \mathrm{f}$ transitions. The integral is over the momentum direction $\boldsymbol{n}_\mathrm{n}$ in the intermediate state, and the summation is over the full set of baryon quantum numbers B_n, including N and Δ states. The prefactor in Eq. (25) is specific to our convention for the amplitude (see above).

Some comments are in order regarding the inelasticity in the intermediate states of the two-photon exchange amplitude. In the parametric domain considered here, the scattering energy is $\sqrt{s} - m = O(N_c^0)$, so that the intermediate states in principle include baryons with masses $m_B - m = O(N_c^0)$ (N^* states), larger than those of the final states with $m_X - m = O(N_c^{-1})$. However, the electromagnetic couplings of such N^* states to the ground state multiplet are suppressed by $1/\sqrt{N_c}$ relative to those between ground state baryons [27,28]. In leading order of the $1/N_c$ expansion it is thus justified to retain only ground state baryons N and Δ as intermediate states. Note also that the two-photon exchange amplitude Eq. (25) is free of collinear divergences, because the large-N_c baryon currents in the $\mathrm{i} \to \mathrm{n}$ and $\mathrm{n} \to \mathrm{f}$ amplitudes satisfy the transversality conditions without corrections in $1/N_c$ [10].

2.3. Cross section

The cross section for inclusive eN scattering Eq. (1) in the $1/N_c$ expansion in the domain Eq. (10) and (11) is obtained from the amplitude Eq. (15) as

$$\frac{d\sigma}{d\Omega_\mathrm{f}} = \frac{1}{16\pi^2} \frac{1}{2} \sum_\lambda \sum_{S_{3\mathrm{i}} S'_{3\mathrm{i}}} \rho(S_{3\mathrm{i}}, S'_{3\mathrm{i}})$$

$$\times \sum_{B_\mathrm{f}} M^*_\mathrm{fi}(\lambda, B_\mathrm{f}, B'_\mathrm{i})\, M_\mathrm{fi}(\lambda, B_\mathrm{f}, B_\mathrm{i}). \tag{26}$$

We write the cross section as differential in the solid angle of $\boldsymbol{n}_\mathrm{f}$, similar to elastic scattering. The inclusive scattering is expressed through the summation over the final baryon states $B_\mathrm{f} = N, \Delta$. The initial baryon is a nucleon, $B_\mathrm{i} = \{\frac{1}{2}, S_{3\mathrm{i}}, I_{3\mathrm{i}}\}$ and $B'_\mathrm{i} = \{\frac{1}{2}, S'_{3\mathrm{i}}, I_{3\mathrm{i}}\}$, with $I_{3\mathrm{i}} = \pm\frac{1}{2}$ for proton/neutron. The spin projections are averaged with the nucleon spin density matrix ρ, normalized as $\mathrm{tr}\,\rho = 1$, which consists of an unpolarized and a polarized part, $\rho = \rho_U + \rho_N$. The unpolarized part is

$$\rho_U = \frac{1}{2}\delta(S_{3\mathrm{i}}, S'_{3\mathrm{i}}). \tag{27}$$

In the case of polarization along the unit vector $\boldsymbol{e}_N$, Eq. (3), the polarized part is (σ^k are the Pauli matrices)

$$\rho_N = \frac{1}{2} e^k_N \sigma^k(S_{3\mathrm{i}}, S'_{3\mathrm{i}}), \tag{28}$$

such that the expectation value of the spin operator is

$$\sum_{S'_{3\mathrm{i}} S_{3\mathrm{i}}} \rho_N(S_{3\mathrm{i}}, S'_{3\mathrm{i}})\, \langle S'_{3\mathrm{i}}|\, \hat{S}^k\, |S_{3\mathrm{i}}\rangle = \frac{1}{2} e^k_N. \tag{29}$$

The spin-independent cross section of Eq. (2) is obtained from the product of e^2 amplitudes in Eq. (26) (see Fig. 1a),

$$\frac{d\sigma_U}{d\Omega_\mathrm{f}} = \frac{1}{16\pi^2}\,\frac{1}{2}\sum_\lambda \sum_{S'_{3\mathrm{i}} S_{3\mathrm{i}}} \rho_U \sum_{B_\mathrm{f}} M^{(e2)*}_\mathrm{fi} M^{(e2)}_\mathrm{fi}; \tag{30}$$

the expression will be evaluated further below. For the spin-dependent cross section, one can easily verify that it is zero at the same order in e^2, because the e^2 amplitude is real and the average with Eq. (28) requires an imaginary part in one of the amplitudes [11,12]. The spin-dependent cross section appears instead from the product of e^2 and e^4 amplitudes, i.e., the interference of one- and two-photon exchange (see Fig. 1b)

$$\frac{d\sigma_N}{d\Omega_\mathrm{f}} = \frac{1}{16\pi^2}\,\frac{1}{2}\sum_\lambda \sum_{S'_{3\mathrm{i}} S_{3\mathrm{i}}} \rho_N \times \sum_{B_\mathrm{f}} \Big[M^{(e2)*}_\mathrm{fi} M^{(e4)}_\mathrm{fi} + M^{(e4)*}_\mathrm{fi} M^{(e2)}_\mathrm{fi} \Big]. \tag{31}$$

With the e^4 amplitude given by Eq. (25), the spin-dependent cross section is completely expressed in terms of the e^2 amplitude Eq. (18), and thus in terms of the large-N_c baryon current matrix elements.

3. Results

3.1. Spin-dependent cross section and asymmetry

We now extract the leading $1/N_c$ term of the spin-dependent cross section. It results from the isovector magnetic current Eq. (23) proportional to the spin-flavor generator $\hat{G}^{i3}$. The e^2 amplitude Eq. (18) produced by this current is

$$M^{(e2)}_\mathrm{fi} = \frac{e^2 F(t_\mathrm{fi})}{1 - \boldsymbol{n}_\mathrm{f}\boldsymbol{n}_\mathrm{i}}\, b^i_\mathrm{fi} \langle B_\mathrm{f}|\hat{G}^{i3}|B_\mathrm{i}\rangle, \tag{32}$$

$$b^i_\mathrm{fi} \equiv i\epsilon^{ijk}(n_\mathrm{f} - n_\mathrm{i})^j \frac{j^k_\mathrm{fi}}{2k}, \tag{33}$$

where j^k_fi is the spatial part of the electron current Eq. (20). The product of e^2 and e^4 amplitudes in Eq. (31) then becomes

$$M^{(e2)*}_\mathrm{fi} M^{(e4)}_\mathrm{fi} = \frac{ie^6 k}{4\pi} \int \frac{d\Omega_\mathrm{n}}{4\pi} \frac{F_\mathrm{fi} F_\mathrm{fn} F_\mathrm{ni}\, b^{k*}_\mathrm{fi}\, b^j_\mathrm{fn}\, b^i_\mathrm{ni}}{(1 - \boldsymbol{n}_\mathrm{f}\boldsymbol{n}_\mathrm{i})(1 - \boldsymbol{n}_\mathrm{f}\boldsymbol{n}_\mathrm{n})(1 - \boldsymbol{n}_\mathrm{n}\boldsymbol{n}_\mathrm{i})} \times \sum_{B_\mathrm{f}} \sum_{B_\mathrm{n}} \langle B'_\mathrm{i}|\hat{G}^{k3}|B_\mathrm{f}\rangle \langle B_\mathrm{f}|\hat{G}^{j3}|B_\mathrm{n}\rangle \langle B_\mathrm{n}|\hat{G}^{i3}|B_\mathrm{i}\rangle, \tag{34}$$

where $F_\mathrm{fi} \equiv F(t_\mathrm{fi})$, etc. It represents a sequence of isovector magnetic transitions, with a tensor structure governed by the electron current and the transition geometry. We evaluate it using algebraic methods based on t-channel angular momentum considerations. For the intermediate states in the e^4 amplitude, we sum over $B_\mathrm{n} = N + \Delta$ using the completeness relation in the ground state representation,

$$\sum_{B_\mathrm{n}} |B_\mathrm{n}\rangle\langle B_\mathrm{n}| = 1, \tag{35}$$

and the product in the last line of Eq. (34) becomes

$$\sum_{B_\mathrm{f}} \langle B'_\mathrm{i}|\hat{G}^{k3}|B_\mathrm{f}\rangle \langle B_\mathrm{f}|\hat{G}^{j3}\hat{G}^{i3}|B_\mathrm{i}\rangle. \tag{36}$$

For the final states, we distinguish two cases:

(i) Nucleon final state, $B_\mathrm{f} = N$. In this case the matrix element of $\hat{G}^{j3}\hat{G}^{i3}$ in Eq. (36) is a $\frac{1}{2} \to \frac{1}{2}$ spin transition, and the tensor formed by the operator product can only have t-channel angular momentum $J = 0$ or 1. The $J = 1$ part is antisymmetric in ij and suppressed in $1/N_c$, because the commutator of the operators is $[\hat{G}^{i3}, \hat{G}^{j3}] = O(N_c^0)$. The tensor can therefore be projected on $J = 0$, which in leading order in $1/N_c$ gives

$$\hat{G}^{j3}\hat{G}^{i3} \to \frac{1}{3}\,\delta^{ji}\,\hat{G}^{l3}\hat{G}^{l3} = \frac{1}{3}\,\delta^{ji}\,\frac{N_c^2}{16}, \tag{37}$$

and Eq. (36) becomes

$$\frac{1}{3}\delta^{ji}\,\frac{N_c^2}{16}\,\langle B'_\mathrm{i}|\hat{G}^{k3}|B_\mathrm{i}\rangle. \tag{38}$$

(ii) Sum of nucleon and Delta final states, $B_\mathrm{f} = N + \Delta$. In this case the summation over B_f can be performed with the completeness relation, see Eq. (35), and Eq. (36) becomes

$$\langle B'_\mathrm{i}|\hat{G}^{k3}\hat{G}^{j3}\hat{G}^{i3}|B_\mathrm{i}\rangle \;\equiv\; T^{kji}. \tag{39}$$

Because the commutator of the $\hat{G}^{i3}$ operators is suppressed in $1/N_c$, see above, the tensor T^{kji} can be regarded as completely symmetric in leading order. As such it can be projected on overall $J = 1$ using

$$T^{kji} \;\to\; \frac{1}{5}(\delta^{kj}T^i + \delta^{ki}T^j + \delta^{ji}T^k), \tag{40}$$

$$T^k \;\equiv\; T^{kll} \;=\; \frac{N_c^2}{16}\,\langle B'_\mathrm{i}|\hat{G}^{k3}|B_\mathrm{i}\rangle. \tag{41}$$

The two cases thus lead to similar contractions of the tensor Eq. (36). The remaining matrix element of $\hat{G}^{k3}$ in Eqs. (38) and (41) is proportional to the initial nucleon spin and isospin, and in leading order of $1/N_c$ evaluates to

$$\langle B'_\mathrm{i}|\hat{G}^{k3}|B_\mathrm{i}\rangle = \frac{N_c}{6}\,\langle S'_{3\mathrm{i}}|\hat{S}^k|S_{3\mathrm{i}}\rangle\,(2I_{3\mathrm{i}}), \tag{42}$$

which can be averaged with the spin density matrix using Eq. (29). Altogether, we obtain the spin-dependent cross section in leading order of $1/N_c$

$$\frac{d\sigma_N}{d\Omega_\mathrm{f}} = \frac{(2I_{3\mathrm{i}})\,\alpha^3 N_c^3 k\, F_\mathrm{fi}}{96\,(1 - \boldsymbol{n}_\mathrm{f}\boldsymbol{n}_\mathrm{i})} \int \frac{d\Omega_\mathrm{n}}{4\pi} \frac{F_\mathrm{fn} F_\mathrm{ni}\,\Phi}{(1 - \boldsymbol{n}_\mathrm{f}\boldsymbol{n}_\mathrm{n})(1 - \boldsymbol{n}_\mathrm{n}\boldsymbol{n}_\mathrm{i})}, \tag{43}$$

$$\Phi = \mathrm{Re}\,\frac{1}{2}\sum_\lambda \frac{i}{3} e_N^k b_{\rm fi}^{k*} b_{\rm fn}^l b_{\rm ni}^l \quad \text{(for } N \text{ final state)}, \tag{44}$$

$$\Phi = \mathrm{Re}\,\frac{1}{2}\sum_\lambda \frac{i}{5} e_N^k \left(b_{\rm fi}^{k*} b_{\rm fn}^l b_{\rm ni}^l + b_{\rm fi}^{l*} b_{\rm fn}^k b_{\rm ni}^l + b_{\rm fi}^{l*} b_{\rm fn}^l b_{\rm ni}^k \right)$$
$$\text{(for } N+\Delta \text{ final state)}. \tag{45}$$

Here $\alpha \equiv e^2/4\pi$ is the fine structure constant. The angular functions Φ can be evaluated using the explicit form of the axial vectors $b_{\rm fi}^i$ etc., Eq. (33). The spin-dependent cross section Eq. (43) is proportional to the initial nucleon isospin $(2I_{3i}) = \pm 1$ and has different sign for ep and en scattering

$$d\sigma_N = d\sigma_N[ep] = -d\sigma_N[en]. \tag{46}$$

We also compute the spin asymmetry

$$A_N \equiv \frac{d\sigma_N}{d\Omega_{\rm f}} \Big/ \frac{d\sigma_U}{d\Omega_{\rm f}}, \tag{47}$$

by dividing by the unpolarized cross section computed in the same approximation. In leading order of $1/N_c$, the unpolarized cross section Eq. (30) arises from the isovector magnetic current in the e^2 amplitude. In the case of summation over N and Δ final states, $B_{\rm f} = N + \Delta$, the result is

$$\frac{d\sigma_U}{d\Omega_{\rm f}} = \frac{\alpha^2 N_c^2 F_{\rm fi}^2}{24\,(1 - \boldsymbol{n}_{\rm f}\boldsymbol{n}_{\rm i})^2} \frac{1}{2}\sum_\lambda b_{\rm fi}^{i*} b_{\rm fi}^i \tag{48}$$

$$= \frac{\alpha^2 N_c^2\,(3 - \boldsymbol{n}_{\rm f}\boldsymbol{n}_{\rm i})\,F_{\rm fi}^2}{48\,(1 - \boldsymbol{n}_{\rm f}\boldsymbol{n}_{\rm i})}. \tag{49}$$

The spin-independent cross section in this approximation is independent of the initial nucleon isospin; the asymmetry Eq. (47) therefore has the same isospin dependence as the spin-dependent cross section in the numerator,

$$A_N = A_N[ep] = -A_N[en]. \tag{50}$$

Some comments on these result from the perspective of the $1/N_c$ expansion are in order. First, the spin-dependent cross section is parametrically large in N_c, as it arises from the maximal product of isovector magnetic currents with matrix elements $O(N_c)$. Second, our calculation provides an example of the "$I = J$ rule" of large-N_c QCD, according to which leading structures appear with t-channel quantum numbers $I = J$ [29–31]. The spin-dependent cross section, as a matrix element between the initial nucleon states $\langle B_{\rm f}^\prime | \ldots | B_{\rm i} \rangle$, is a structure with overall $J = 1$, and its leading large-N_c result has $I = 1$. It arises as the product of an e^2 amplitude with $I = J = 1$ (for both N and Δ final states) with an e^4 amplitude that is either projected on $I = J = 0$ (for N final) or on $I = J = 2$ (for Δ final), as can be observed in the algebraic calculation above.

3.2. Numerical results

We now evaluate the asymmetry numerically and study its kinematic dependence using the leading-order $1/N_c$ expansion results, Eqs. (43)–(45) and Eq. (49). The large-N_c form factors $F(t)$ appearing in the expressions are fixed by the matching condition Eq. (24), and we use the standard dipole form $(1 - t/0.71\,\mathrm{GeV}^2)^{-2}$ to model the empirical t-dependence.

Fig. 2 shows A_N for two values of the CM momentum k, as a function of the CM scattering angle $\theta = \mathrm{angle}(\boldsymbol{n}_{\rm f}\boldsymbol{n}_{\rm i})$. Results are shown for the cases of N and $N + \Delta$ final states in σ_N in the numerator; σ_U in the denominator is always for $N + \Delta$ final states;

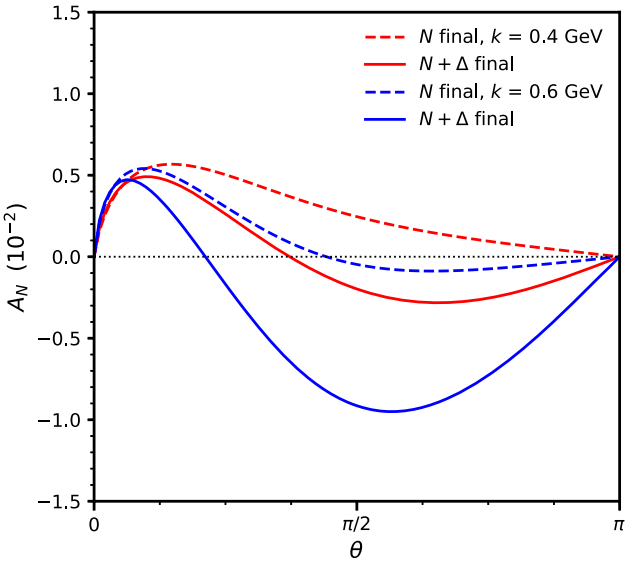

Fig. 2. Target normal single-spin asymmetry A_N in inclusive eN scattering, Eq. (47), in leading order of the $1/N_c$ expansion, for two values of the CM momentum k, as a function of the CM scattering angle θ. *Dashed lines:* A_N with N final state in σ_N in the numerator. *Solid lines:* A_N with $N + \Delta$ final states in σ_N. In both cases, σ_U in the denominator is with $N + \Delta$ final states.

in this way one can add/subtract the results for A_N in the graph and see the contributions of the various channels to σ_N. (The intermediate states in the two-photon exchange amplitude in σ_N are always the sum $N + \Delta$.)

One observes: (i) A_N vanishes at $\theta = 0$ and π, which is natural, as at these angles the normal vector $\boldsymbol{n}_2 \times \boldsymbol{n}_1$ vanishes. (ii) The contribution of Δ final states (the difference of the results for $N + \Delta$ and N final states) is small at small θ but becomes significant at $\theta \sim \pi/2$, causing the A_N for final $N + \Delta$ to be several times larger than that for final N. (iii) A_N reaches values $\sim 10^{-2}$ at $\theta \sim \pi/2$ and $k \sim 0.6$ GeV.

Some comments on the region of applicability of the large-N_c expressions are in order. (i) The $1/N_c$ expansion in the domain Eq. (11) assumes that the Δ channel is open. The expressions should therefore be applied at CM energies above the physical Δ threshold $\sqrt{s} = 1.23$ GeV. (ii) The calculation relies on the $1/N_c$ suppression of N^* states with masses $m_B - m = O(N_c^0)$ as intermediate states in the two-photon exchange amplitude. This should be reasonable at energies up to and moderately above the N^* threshold $\sqrt{s} \sim 1.5$ GeV, but not substantially above it. (iii) The leading-order results for σ_N and A_N arise entirely from magnetic currents, which are proportional to the momentum transfers at the vertices. They are not expected to be accurate at small $\theta \ll \pi/2$ and $k \ll 1$ GeV, where the momentum transfers are kinematically suppressed and contributions from electric currents are important (those can be computed as part of the $1/N_c$ corrections). Altogether, we expect the leading-order $1/N_c$ result to be a fair approximation at CM momenta $k \sim$ 0.3–0.6 GeV and large angles $\theta \sim \pi/2$. In this kinematics the accuracy of the leading-order $1/N_c$ result is naively estimated to be of the order $\sim 1/3$, as observed in other hadronic observables. A more quantitative assessment of the accuracy will become possible with the computation of $1/N_c$ corrections.

We note that the numerical results for σ_N and A_N in the $1/N_c$ expansion are strongly affected by the presence of the form factors in the integral in Eq. (43). This indicates that the two-photon exchange observables are sensitive to baryon structure in the domain considered here.

4. Extensions

We have studied the target normal single-spin asymmetry in inclusive eN scattering in leading order of the $1/N_c$ expansion, in the parametric domain where the energy transfer is $O(N_c^{-1})$ and allows for Δ excitation, and the momentum transfer is $O(N_c^0)$ and probes the internal structure of the baryons. The results can be extended and applied in several ways.

The method developed here, particularly the algebraic approach in Sec. 3, can be used to compute $1/N_c$ corrections to the leading-order result. These corrections will quantify the numerical accuracy of the leading-order result for the isovector σ_N, and provide estimates of the isoscalar σ_N, which appears only at subleading order.

In the parametric domain considered here, the intermediate states in the two-photon exchange amplitude have energies $\sqrt{s} - m = O(N_c^0)$ and include N^* baryons with masses $m_B - m = O(N_c^0)$. In the present analysis we have neglected such intermediate states because their electromagnetic couplings to the initial/final N and Δ states are suppressed by factors $1/\sqrt{N_c}$. When such N^* states are included, they can enhance the region of quasi-real photon exchange (collinear to the electron momenta) in the two-photon exchange integral, which could result in numerically enhanced contributions. This effect needs to be analyzed in the context of the higher-order $1/N_c$ expansion.

The cross section for inclusive eN scattering includes also real photon emission into the final state (Fig. 1c). This process can be analyzed in the $1/N_c$ expansion in the same manner as two-photon exchange (Fig. 1b). If the intermediate state is a Δ, the emitted photon momentum is $k_\gamma = O(N_c^{-1})$, because its energy is given by the mass difference $m_\Delta - m = O(N_c^{-1})$. In this situation the coupling through the leading magnetic vertex is suppressed, and we expect real photon emission to be suppressed in leading order of the $1/N_c$ expansion. If the intermediate state is an N^* with mass difference $m_B - m = O(N_c^0)$, as becomes possible in higher orders in $1/N_c$, the emitted photon momentum is $k_\gamma = O(N_c^0)$, and real emission can contribute at the same order as two-photon exchange. The higher-order $1/N_c$ expansion therefore needs to treat two-photon exchange and real photon emission on the same basis. Overall, the parametric expansion in $1/N_c$ provides definite prescriptions for including both N^* excitation and real photon emission in the inclusive normal single-spin asymmetry.

The $1/N_c$ expansion can also be performed in parametric domains different from Eqs. (10) and (11). For example, the choice $k = O(N_c^{-1})$ leads to a "low-energy expansion" in which the electric currents enter in the same order as the magnetic ones, giving rise to a different physical picture.

The framework of the $1/N_c$ expansion can also be used to explore the transition between the resonance and DIS regions and the realization of quark-hadron duality in two-photon exchange observables. Theoretical estimates of A_N differ by 1-2 orders of magnitude between the resonance and DIS regions, because of the large effects of the anomalous magnetic moment that are present in resonance production but disappear in DIS [10,15–17]. Performing $1/N_c$ expansions in different kinematic domains would help explain how the transition happens.

The methods developed here can be applied to the beam spin asymmetry in eN scattering, a two-photon exchange effect proportional to the electron mass, which is being studied as a background to parity-violating electron scattering [32–34].

This material is based upon work supported by the U.S. Department of Energy Office of Science, Office of Nuclear Physics under contract DE-AC05-06OR23177 (JLG, CWe); by the National Science Foundation, Grant Number PHY 1913562 (JLG); and by the Fonds de la Recherche Scientifique (FNRS) (Belgium), Grant Number4.45.10.08 (CTWi).

Declaration of competing interest

The authors declare that they have no known competing financial interests or personal relationships that could have appeared to influence the work reported in this paper.

Data availability

Data will be made available on request.

References

[1] C.E. Carlson, M. Vanderhaeghen, Two-photon physics in hadronic processes, Annu. Rev. Nucl. Part. Sci. 57 (2007) 171–204, https://doi.org/10.1146/annurev.nucl.57.090506.123116, arXiv:hep-ph/0701272.
[2] M.K. Jones, et al., G_{Ep}/G_{Mp} ratio by polarization transfer in $\vec{e}p \to e\vec{p}$, Phys. Rev. Lett. 84 (2000) 1398–1402, https://doi.org/10.1103/PhysRevLett.84.1398, arXiv:nucl-ex/9910005.
[3] P.A.M. Guichon, M. Vanderhaeghen, How to reconcile the Rosenbluth and the polarization transfer method in the measurement of the proton form-factors, Phys. Rev. Lett. 91 (2003) 142303, https://doi.org/10.1103/PhysRevLett.91.142303, arXiv:hep-ph/0306007.
[4] P.G. Blunden, W. Melnitchouk, J.A. Tjon, Two photon exchange and elastic electron proton scattering, Phys. Rev. Lett. 91 (2003) 142304, https://doi.org/10.1103/PhysRevLett.91.142304, arXiv:nucl-th/0306076.
[5] B.S. Henderson, et al., Hard two-photon contribution to elastic lepton-proton scattering: determined by the OLYMPUS experiment, Phys. Rev. Lett. 118 (9) (2017) 092501, https://doi.org/10.1103/PhysRevLett.118.092501, arXiv:1611.04685.
[6] J.C. Bernauer, et al., Measurement of the charge-averaged elastic lepton-proton scattering cross section by the OLYMPUS experiment, Phys. Rev. Lett. 126 (16) (2021) 162501, https://doi.org/10.1103/PhysRevLett.126.162501, arXiv:2008.05349.
[7] A. Accardi, et al., An experimental program with high duty-cycle polarized and unpolarized positron beams at Jefferson lab, Eur. Phys. J. A 57 (8) (2021) 261, https://doi.org/10.1140/epja/s10050-021-00564-y, arXiv:2007.15081.
[8] E. Cline, et al., Characterization of muon and electron beams in the Paul Scherrer Institute PiM1 channel for the MUSE experiment, arXiv:2109.09508, 2021.
[9] A.V. Afanasev, C.E. Carlson, Two-photon-exchange correction to parity-violating elastic electron-proton scattering, Phys. Rev. Lett. 94 (2005) 212301, https://doi.org/10.1103/PhysRevLett.94.212301, arXiv:hep-ph/0502128.
[10] A. Afanasev, M. Strikman, C. Weiss, Transverse target spin asymmetry in inclusive DIS with two-photon exchange, Phys. Rev. D 77 (2008) 014028, https://doi.org/10.1103/PhysRevD.77.014028, arXiv:0709.0901.
[11] A.O. Barut, C. Fronsdal, Spin-orbit correlations in μ–e and e^-–e^- scattering, Phys. Rev. 120 (1960) 1871–1874, https://doi.org/10.1103/PhysRev.120.1871.
[12] N. Christ, T.D. Lee, Possible tests of C_{st} and T_{st} invariances in $l^\pm + N \to l^\pm + \Gamma$ and $A \to B + e^+ + e^-$, Phys. Rev. 143 (1966) 1310–1321, https://doi.org/10.1103/PhysRev.143.1310.
[13] A. Airapetian, et al., Search for a two-photon exchange contribution to inclusive deep-inelastic scattering, Phys. Lett. B 682 (2010) 351–354, https://doi.org/10.1016/j.physletb.2009.11.041, arXiv:0907.5369.
[14] J. Katich, et al., Measurement of the target-normal single-spin asymmetry in deep-inelastic scattering from the reaction $^3\mathrm{He}^\uparrow(e,e')X$, Phys. Rev. Lett. 113 (2) (2014) 022502, https://doi.org/10.1103/PhysRevLett.113.022502, arXiv:1311.0197.
[15] A. Metz, M. Schlegel, K. Goeke, Transverse single spin asymmetries in inclusive deep-inelastic scattering, Phys. Lett. B 643 (2006) 319–324, https://doi.org/10.1016/j.physletb.2006.11.009, arXiv:hep-ph/0610112.
[16] A. Metz, D. Pitonyak, A. Schafer, M. Schlegel, W. Vogelsang, J. Zhou, Single-spin asymmetries in inclusive deep inelastic scattering and multiparton correlations in the nucleon, Phys. Rev. D 86 (2012) 094039, https://doi.org/10.1103/PhysRevD.86.094039, arXiv:1209.3138.
[17] M. Schlegel, Partonic description of the transverse target single-spin asymmetry in inclusive deep-inelastic scattering, Phys. Rev. D 87 (3) (2013) 034006, https://doi.org/10.1103/PhysRevD.87.034006, arXiv:1211.3579.
[18] G.N. Grauvogel, T. Kutz, A. Schmidt, Target-normal single spin asymmetries measured with positrons, Eur. Phys. J. A 57 (6) (2021) 213, https://doi.org/10.1140/epja/s10050-021-00531-7, arXiv:2103.05205.
[19] G. 't Hooft, A planar diagram theory for strong interactions, Nucl. Phys. B 72 (1974) 461, https://doi.org/10.1016/0550-3213(74)90154-0.
[20] E. Witten, Baryons in the $1/N$ expansion, Nucl. Phys. B 160 (1979) 57–115, https://doi.org/10.1016/0550-3213(79)90232-3.
[21] J.-L. Gervais, B. Sakita, Large-N QCD baryon dynamics: exact results from its relation to the static strong coupling theory, Phys. Rev. Lett. 52 (1984) 87, https://doi.org/10.1103/PhysRevLett.52.87.
[22] J.-L. Gervais, B. Sakita, Large-N baryonic soliton and quarks, Phys. Rev. D 30 (1984) 1795, https://doi.org/10.1103/PhysRevD.30.1795.

[23] R.F. Dashen, A.V. Manohar, Baryon-pion couplings from large-N_c QCD, Phys. Lett. B 315 (1993) 425–430, https://doi.org/10.1016/0370-2693(93)91635-Z, arXiv:hep-ph/9307241.
[24] R.F. Dashen, E.E. Jenkins, A.V. Manohar, $1/N_c$ expansion for baryons, Phys. Rev. D 49 (1994) 4713, https://doi.org/10.1103/PhysRevD.51.2489, Erratum: Phys. Rev. D 51 (1995) 2489, arXiv:hep-ph/9310379.
[25] R.F. Dashen, E.E. Jenkins, A.V. Manohar, Spin flavor structure of large N_c baryons, Phys. Rev. D 51 (1995) 3697–3727, https://doi.org/10.1103/PhysRevD.51.3697, arXiv:hep-ph/9411234.
[26] I.P. Fernando, J.L. Goity, $SU(3)$ vector currents in baryon chiral perturbation theory combined with the $1/N_c$ expansion, Phys. Rev. D 101 (5) (2020) 054026, https://doi.org/10.1103/PhysRevD.101.054026, arXiv:1911.00987.
[27] J.L. Goity, $1/N_c$ countings in baryons, Phys. At. Nucl. 68 (2005) 624–633, https://doi.org/10.1134/1.1903092, arXiv:hep-ph/0405304.
[28] J.L. Goity, $1/N_c$ countings in baryons: mixings and decays, in: ECT* Workshop on Large Nc QCD 2004, 2005, pp. 211–222, arXiv:hep-ph/0504121, https://doi.org/10.1142/9789812701725_0014.
[29] M.P. Mattis, The $I_t = J_t$ rule in action, Phys. Rev. D 39 (1989) 994–997, https://doi.org/10.1103/PhysRevD.39.994.
[30] M.P. Mattis, M. Mukherjee, The $I_t = J_t$ rule: a new large N_c selection rule for meson-baryon scattering, Phys. Rev. Lett. 61 (1988) 1344, https://doi.org/10.1103/PhysRevLett.61.1344.
[31] R.F. Lebed, The large N_c baryon-meson $I_t = J_t$ rule holds for three flavors, Phys. Lett. B 639 (2006) 68–73, https://doi.org/10.1016/j.physletb.2006.06.014, arXiv:hep-ph/0603150.
[32] A.V. Afanasev, N.P. Merenkov, Collinear photon exchange in the beam normal polarization asymmetry of elastic electron-proton scattering, Phys. Lett. B 599 (2004) 48, https://doi.org/10.1016/j.physletb.2004.08.023, arXiv:hep-ph/0407167.
[33] C.E. Carlson, B. Pasquini, V. Pauk, M. Vanderhaeghen, Beam normal spin asymmetry for the $ep \to e\Delta(1232)$ process, Phys. Rev. D 96 (11) (2017) 113010, https://doi.org/10.1103/PhysRevD.96.113010, arXiv:1708.05316.
[34] O. Koshchii, A. Afanasev, Lepton mass effects for beam-normal single-spin asymmetry in elastic muon-proton scattering, Phys. Rev. D 100 (9) (2019) 096020, https://doi.org/10.1103/PhysRevD.100.096020, arXiv:1905.10217.